Design and Performance of a Prototype Tactile Shape Display for Minimally Invasive Surgery

Maria V. Ottermo[1,2], Øyvind Stavdahl[1] and Tor A. Johansen[1]
[1] Norwegian University of Science and Technology,
Department of Engineering Cybernetics
[2] SINTEF IKT Applied Cybernetics
Trondheim, Norway
maria.v.ottermo@sintef.no
{oyvind.stavdahl, tor.arne.johansen}@itk.ntnu.no

Abstract

The design of a tactile shape display intended for Minimally Invasive Surgery (MIS) is presented. It consists of 32 micro brushless motors arranged in a 4-by-8 configuration, and the total size is 27 mm $\times$ 20 mm $\times$ 18 mm. The main restrictive design parameter is the size of the display as it will be attached to a laparoscopic grasper. Modularity is also crucial since it might be desirable to do experiments with other pins or effectors attached to the actuators. The tactel (TACTile ELement) spacing is 2.7 mm with a tactel diameter of maximum 2.6 mm. The display is tested with respect to pin force, positioning accuracy, bandwidth and stiffness. Results show that the tactels can provide an active force of 0.4-0.5 N at a frequency of close to 0.7 Hz at full excursion (3 mm). The testing also show that positioning accuracy is approximately 40 μm, while the stiffness is close to 50 N/mm.

1 Introduction

Tactile feedback is critical for dexterous motor control. Without it, we drop objects and have trouble using different tools. Moreover, when spatial tactile information is unavailable, substantial decrease in performance is observed for most sensory and perceptual tasks [11].

Tactile displays are devices built to convey small scale spatial information about objects that cannot be directly manipulated by the user. These devices are believed to have a wide variety of applications, including computer interaction, minimally invasive surgery, and exploration tasks in general.

In laparoscopic surgery, the operation is performed with instruments and viewing equipment inserted into the body through small incisions created by the surgeon. This method has many advantages, including minimization of surgical trauma and damage to healthy tissue. However, laparoscopic surgery requires specialized dexterity even beyond that needed for open surgery. Reduced tactile feedback, different eye-hand coordination, and translation of a two-dimensional video image into a three-dimensional working area are just some of the obstacles in the performance of laparoscopic surgery. The lack of tactile feedback limits the surgeon's abilities to palpate internal organs, a technique actively used for locating tumors, gallstones and abnormalities in the tissue during open surgery. Combining the lack of tactile feedback with poor visual feedback also results in reduced positioning and manipulation control of the instruments. Our remote palpations system is designed to serve as an extension of the surgeon's fingers. A sensor array attached to the instrument's end effector measures contact forces between the array and the tissue, and this tactile information is sent to the surgeon's fingers to provide him with a feeling of the shape or hardness of the tissue.

The somatic senses are the nervous mechanisms that collect sensory information from the body. In particular, the mechanoreceptive somatic senses, which include both tactile and position sensations, are stimulated by the mechanical displacement of some tissue of the body. The tactile senses include touch, pressure and tickle senses, and the body exhibits at least six entirely different types of tactile receptors [6]. The complexity of the tactile sense and the fact that there are still many unanswered questions about human perception have put restrictions on the research on tactile displays, and a satisfactory solution has yet to be found. Several research groups have tried to identify requirements for the ideal tactile display. According to Moy, Wagner and Fearing [14] the force required is 1 N per tactel when the actuator density is 1 per mm^2, with up to 2 mm indentation and a bandwidth > 50 Hz. Peine, Wellman and Howe [21] suggest that the indentation should be 2 to 3 mm with a force between 1 and 2 N per tactel. They also suggest that the bandwidth should be set to 30 Hz to match maximum finger speeds during natural haptic exploration.

Most tactile displays use an array of stimulators in contact with the skin to stimulate mechanoreceptors in the finger tip. Previous designs include use of shape memory alloy [22], pneumatics [13, 14], piezoelectricity [5, 8], voice coils [20], electrical stimulation [10], ultrasound [9] and servomotors [24, 25].

Size, weight and fidelity in pin motion control are often the main limitations for tactile shape displays [22]. In this paper we describe the design of a display that consists of 32 micro motors configured in a 4-by-8 array [18]. The main advantage of the design is the small size. The tactile display described in [26] is also based on small motors and is highly effective, but the size makes it unsuitable for use with a laparoscopic graspers. Compared to some displays that use tendons in the actuator mechanism, for instance [24], our compact design provides very high stiffness. Additionally, the design has a relatively high tactel resolution, and the positioning of the pins is very accurate.

2 Principle and Design

The motors used are of type designation SLB-06H1PG79 by Namiki Precision Jewels. Each motor measures 2.4 mm in diameter and 12 mm in length (including gear head and shaft), see Figure 1. The total weight of the display is 54 g.

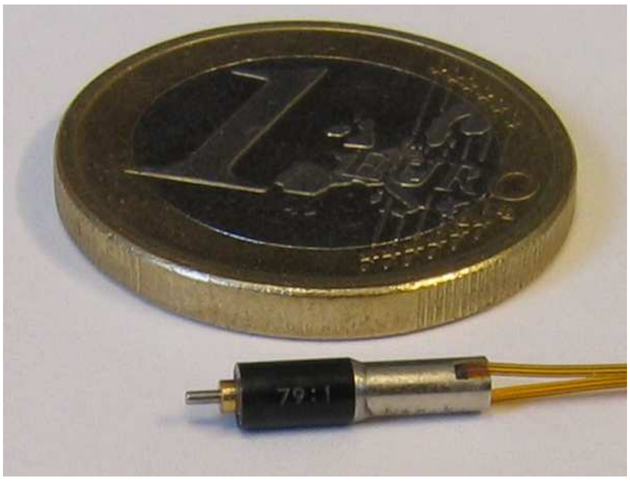

Figure 1: Motor.

The finger is indented vertically and the basic principle is a screw connection attached to the gear head shaft which screws the tactel up and down when the shaft rotates (Figure 2).

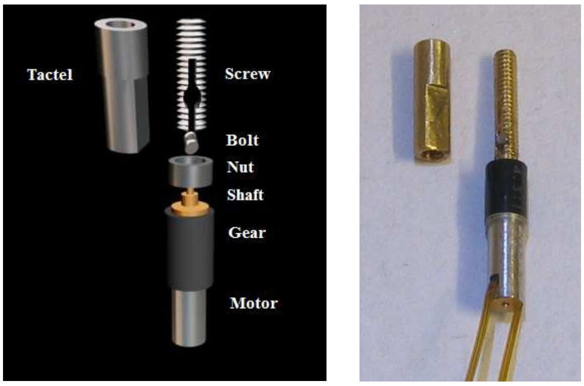

Figure 2: Integration of tactel and motor.

The position setpoint of each tactel is determined by an electric signal, and is a function of the force exerted on a tactile sensor which is attached to the grasper's end-effector.

2.1 Tactile Sensor

The sensory part of the system is not the focus for this paper, but it is described briefly in this section. The tactile sensor array used is a PPS TactArray (Pressure Profile Systems Inc.) developed for measuring the tactile pressure distribution between objects in direct physical contact. It consists of a two-dimensional array (15×4) of pressure sensing capacitive elements in a thin, continuous sheet, and the total size of the array is 35 mm $\times$ 10 mm. Included in the system is software for acquiring, visualizing and storing data. Our system fits onto an Olympus A6998 reusable laparoscopic grasper and covers the area of the grasper jaw in an optimal way (Figure 3). The tactile sensor system has been thoroughly tested in [17].

2.2 Tactel Mechanism

Each pin consists of a motor with gear head and shaft, a mechanism used to attach the screw to the gear head shaft and the tactel top (Figure 2). The mechanism attached to the gear head shaft consists of three small parts; screw, bolt and nut,

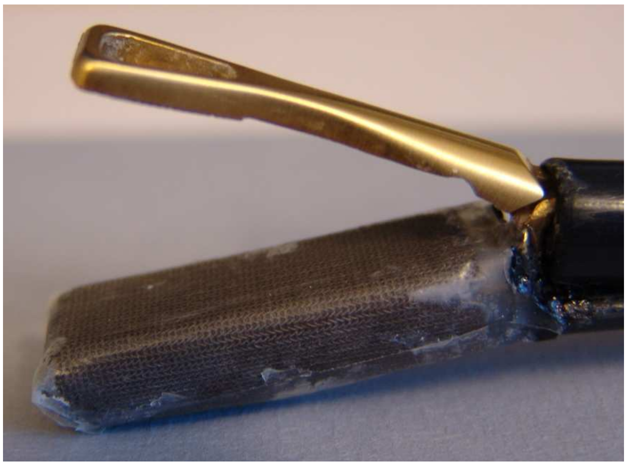

Figure 3: Close-up of a conventional grasper with the sensor array attached.

and this is visualized in the 3D drawing in the left part of Figure 2. The screw has a diameter of 1.4 mm. As the figure shows, a split runs vertically halfway through the screw. Additionally, a hole runs through the screw in the horizontal direction. The bolt is cylindrical with a diameter of 0.8 mm and a length of 1 mm. A hole is drilled through the bolt such that it can be threaded onto the gear head's shaft. The bolt and gear head shaft fit into the screw split and hole, and a nut secures this connection. The advantage of using this mechanism over glue, is that it is more mechanically flexible, and hence will prevent damage to the motor and gear head if exposed to excessive vertical forces. In addition, it is more modular than glue, since it is easier to replace the different parts if any of them should break.

The upper part of the tactel top has a cylindrical shape, while some material is milled off on two opposite sides of the lower part, resulting in two flat sections. These flat sections are the keys to translating the rotational movement of the motor into the linear movement of the tactel. This is described in more detail in Section 2.3. The inner working of the tactel has threads that match those of the screw attached to the gear head shaft. Since the tactels are threaded all the way through, different tops can be screwed onto the tactel, allowing for testing with different effector shapes. Our hypothesis is that the shape and size of the pins greatly affect the way information is rendered on the tactile display, but this will not be further explored in this paper [16].

2.3 Display Housing

The overall design of the display housing is shown in Figure 4, while the actual display is shown in Figure 5.

The display housing consists of four layers stacked together, as shown in Figure 4. Each layer contains 32 holes that match the shapes of the different parts of the tactel mechanism. One of the major challenges of designing the display is that the motors and gear heads are fragile, and hence the display housing must be designed to protect against external forces. An additional problem is that the motor is only loosely attached to the gear head. The motor and the gear head have different diameters, 2 mm and 2.4 mm respectively. By fitting the motor into the lower layer with 2 mm holes and the gear head into the middle layer with 2.4 mm holes, we strengthen the connection between the motor and the gear head, and hence reduce the chance of damage. The layer approach also provides a modular design. The nut that secures the connection between the tactel mechanism and the gear head shaft rests upon the bearing layer, which has holes that match the dimension of the shaft (0.5 mm). This ensures that pressure applied from the finger will be absorbed by the bearing layer rather than the fragile gear heads. The holes of the upper layer have a shape that match that of the tactel described in Section 2.2. This means that the upper part of the hole is cylindrical, while the lower part is shaped as a split. This is illustrated in the lower part of Figure 4, which shows a cross-section of the display. By trapping the flat part of the tactel in this split, the rotational movement is transformed to the linear movement needed to indent the finger vertically.

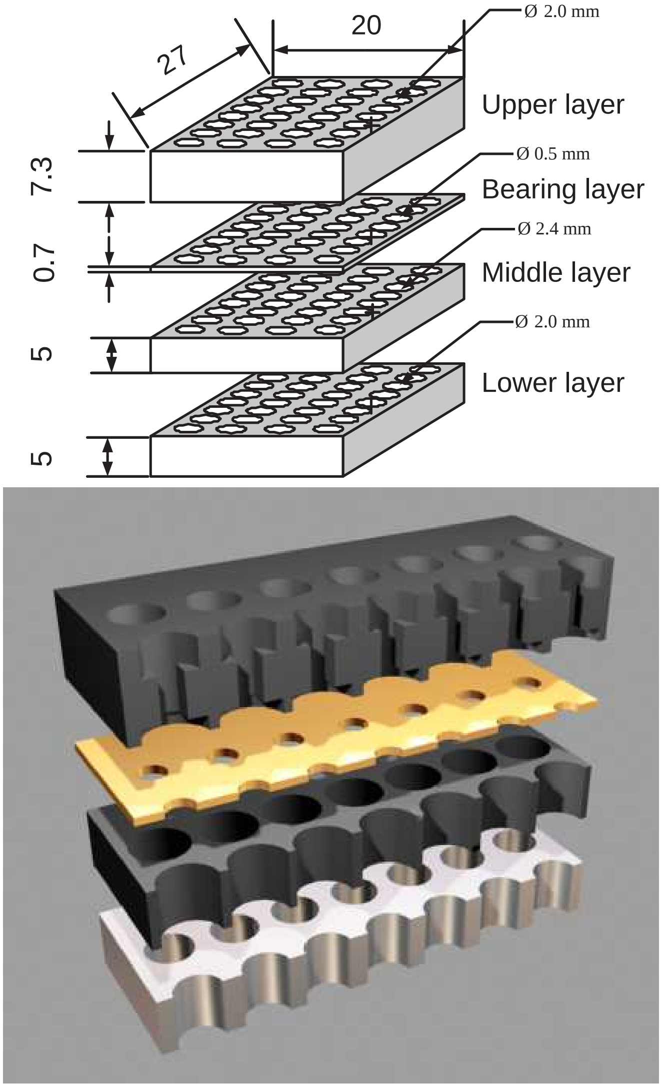

Figure 4: The upper figure shows the overall design and measures of the display (all measures in mm), while the lower figure shows a cross section of the display.

The top and middle layer are made of an acetal resin engineering plastic. For the top layer, this reduces the friction between the tactel mechanism and the housing. The bearing layer is made of metal to absorb the forces applied on the tactel mechanism. To prevent magnetic crosstalk between the motors, the lower layer is made of iron or mu metal (in our case a Permimphy material, which is a Fe-Ni soft magnetic alloy). Mu metal has a permeability close to a 100 times

Figure 5: Display housing, where half of the display is covered by the spatial low pass filter.

higher than iron, and this will increase the torque slightly, since the high permeability adds a positive component to the motor's magnetic field. Both materials are tested in the torque performance tests.

A thin protective layer of silicone rubber is adhered to the top surface of the display (Figure 5). This provides spatial low pass filtering to make discrete pins feel like a single continuous object [12].

Figure 6 illustrates how the display can be attached to a laparoscopic handle. The handle is custom made and integrates both the display and the driver circuits in the handle [15]. This handle design shows the operator touching the tactile display with the thumb. The index finger is the most sensitive finger, and it could be that the sensation of the thumb is not adequate for remote palpation. No tests have been done to examine these issues. However, one can easily picture an alternative design with the display integrated in the moving "trigger" button handled by the index finger. This would integrate the movement of the index finger and the force image sensed by it, thus possibly creating an enhanced, interactive palpation experience.

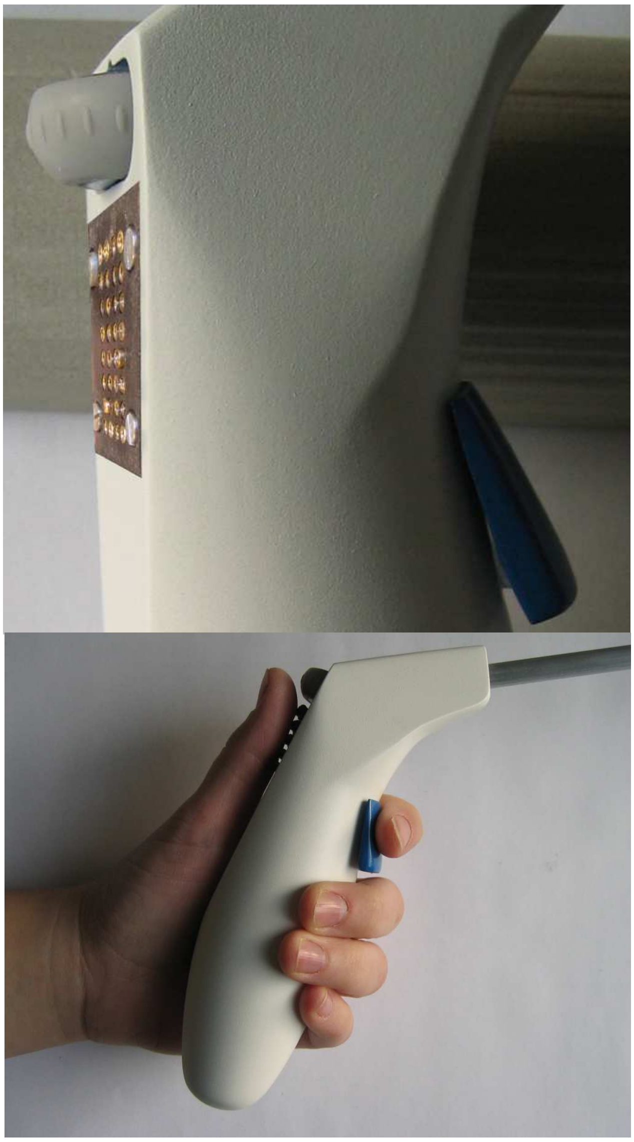

Figure 6: The above figure illustrates how the display can be integrated in a custom made laparoscopic handle. The full laparoscopic instrument is shown at the bottom.

2.4 Driver Circuit

The driver circuit designed to operate the motors is a SSD04 3-phase sensorless driver circuit from Namiki, and this is shown to the right in Figure 8. Since 32 driver circuits are needed, they require too much space. Therefore, a control module that integrates the 32 driver circuits in one block has been designed (left part of Figure 8). The block consists of four cards for motor control and one for connection to PC/Power. The total size is 34 mm$\times$ 34 mm$\times$ 45 mm. The cables from the motors are only 5 cm, and therefore the display has to be mounted close to the driver circuit. Because of this, focus was put on making the driver circuits as light and small as possible. The cables between the driver circuits and the PC can be made fairly long, meaning that both the power source and interface to PC can be separated from the surgical area. There are four cables running from the RS485 interface to the driver circuits, each of which has a diameter of 1 mm. These cables are not stiff, and hence they will not influence the usability of the device much.

Each of the four motor control cards controls 8 motors and contains an FPGA together with driver circuits, circuits for programming of the FPGA, RS485 transceiver and connectors for the motors, see Figure 7. When stacking the cards, the FPGAs are automatically cascaded such that each card can be addressed directly. Although only four cards are used for controlling the 32 motors, it can be expanded to as much as 8 cards, and each card has dedicated addresses in the address space of 256.

Serial communication with a computer is done with Universal Asynchronous Receiver/Transmitter (UART). A 4-wire RS485 enables communication at up to 1 Mbaud over a few meters.

Setpoints for position and acceleration are easily set by the user. The original SSD04 driver circuit uses two phases to control the motor and the third phase as a rotation sensor. The custom made circuit commutates the motor as a stepper motor (dividing one revolution of the motor shaft into six discrete steps), and uses all phases for control. The major advantage of using this stepper motor approach is that it provides the opportunity to accurately dictate the position without having to verify the position with a shaft encoder [7]. The drawback is that the precise and repeatable positioning of the motor shaft comes at the sacrifice of speed capacity. Since the commutation with our circuit is done without feedback,

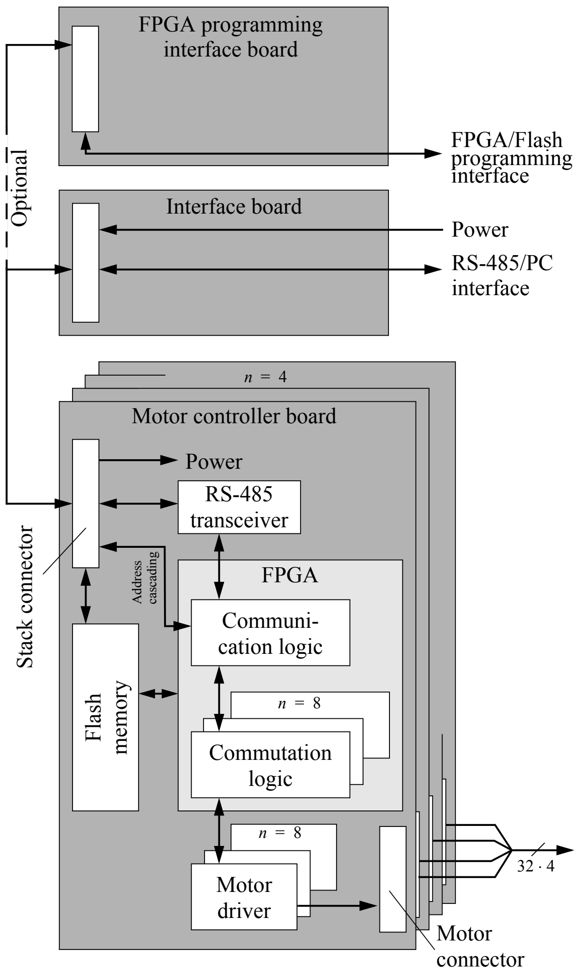

Figure 7: Figure showing a basic schematic of the driver circuit.

we do not know when it is optimal to commutate again, and hence we need to limit the commutation frequency in order to avoid slippage. Our circuit is approximately 49% slower than the original circuit at no load speed. We do, however, assume that this difference is smaller under load, as we have more torque available to drive the load when using our commutation scheme (due to a higher torque constant). Due to inertia in the motors, commutation is done using a speed ramp. This is implemented using a table of 20 elements where each element determines how many periods of 16 MHz will pass between commutations.

With the custom made driver circuit the motor

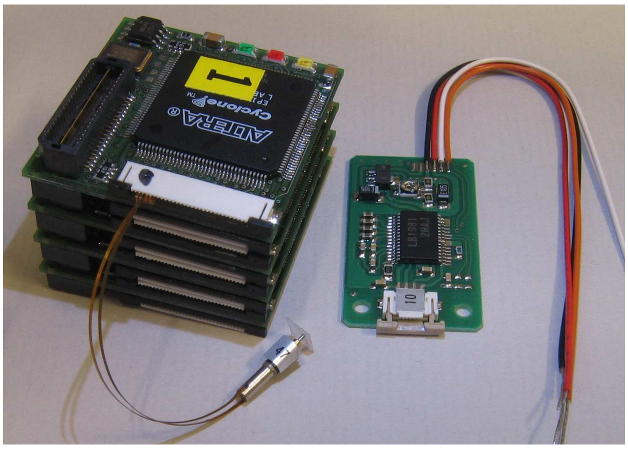

Figure 8: The specially designed driver circuit for 32 motors to the left and the original SSD04 driver circuit to the right.

is run by applying voltage to all three terminals simultaneously, with their common point being ground. +3 V or -3 V is applied to each terminal depending on where the motor is in the commutation cycle, see Figure 9.

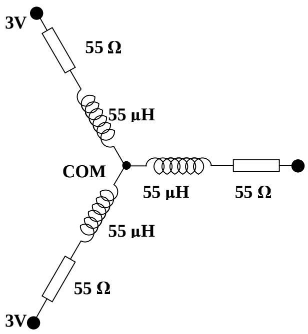

Figure 9: Stator winding configuration and impedances.

At stall (motor is forced to a stop), there is no back-emf and the inductance is irrelevant. Each resistance sees a voltage of 3 V, differing only in direction, causing all phase currents, I_p, to have the same theoretical absolute value:

$$I_p = \frac{3V}{55\Omega} = 54.5mA \tag{1}$$

To find the actual input current, a 1.2Ω resistor was connected in series with one of the motor inputs and the voltage drop measured. The mean voltage drop at stall was approximately 61 mV, corresponding to 53 mA.

The nominal torque constant given by the data sheet is based on normal operation where only two phases are used for the commutation. Since we use three phases we need to calculate a new torque constant, where the new geometry is taken into account. The two cases are compared in Figure 10.

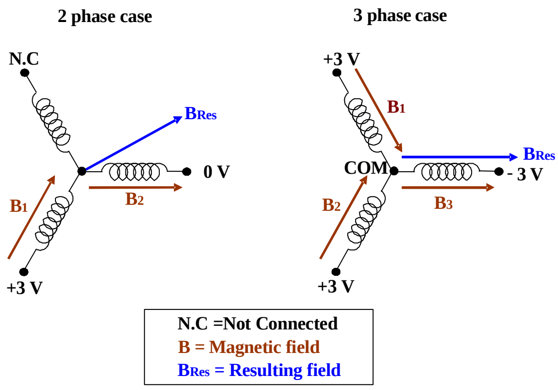

Figure 10: Resulting field when using 2 and 3 active phases, respectively.

With the new estimated torque constant, $K_t = 15\frac{mNm}{A}$, and the measured input current, I_m, we get the torque, T_m, available for driving the load:

$$\begin{aligned} T_m &= T_d - T_{fm} = I_m K_t - T_{fm} \\ &= (15\frac{mNm}{A} \cdot 51mA) - 0.156mNm \\ &= 0.609mNm \end{aligned} \tag{2}$$

where T_d is the developed torque and T_{fm} is the friction torque given by the motor's data sheet.

3 Performance Tests

To evaluate the performance of the tactile display we use the set up shown in Figure 11. The setup consists of a lever arm attached to a rotary potentiometer that is actuated by displacement of the tactel being tested. A plate attached to the end of the lever arm makes it possible to adjust the load exerted on the tactel. The high resolution rotary potentiometer outputs a voltage proportional to the angle of displacement, θ.

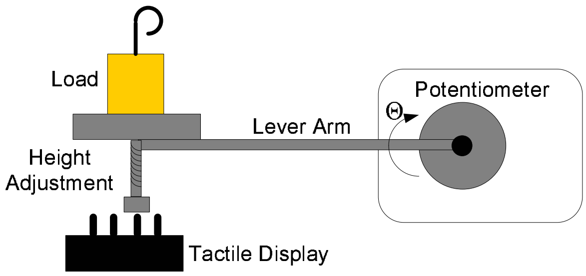

Figure 11: Experimental set up.

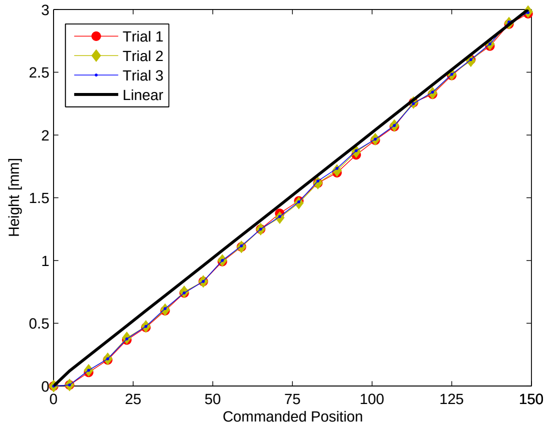

Figure 12: Plot showing commanded position versus height [mm].

3.1 Positioning Accuracy

Each tactel can be given 150 different position setpoints distributed along the maximum excursion of 3 mm. This implies a theoretical positioning resolution of 20 μm. To verify this, a typical tactel was given 25 incremental steps from 0 to 149. The results for three trials are shown in Figure 12. The maximum error between true linear value and pin height was 0.1517 mm, and the standard deviation was 0.0382. This corresponds to a positioning accuracy of approximately 40 μm.

3.2 Force and Bandwidth

To specify the force and bandwidth the display can provide, two typical tactels were stepped from 0 to max excursion ($3\ mm$) and from max excursion to 0, at our maximum speed. With 6 commutations per revolution, a gear head reduction, n, of 79:1 and a minimum of 10 periods of $16\ MHz$ between commutations, we have a maximum speed, $v_{rps} = 1041 rps$, which with a thread pitch, $p = 0.3\ mm/round$, corresponds to:

$$\begin{aligned} v &= \frac{v_{rps} p}{n} = \frac{1041\ rps}{79} \cdot 0.3\ \frac{mm}{round} \\ &= 4\ \frac{mm}{s} \end{aligned} \tag{3}$$

The results showed that the fall time was 0.7 s and the rise time 0.76 s, which gives us a bandwidth of approximately 0.68 Hz. This corresponds well with theory:

$$f = \frac{v}{(2h_{max})} = \frac{4\frac{mm}{s}}{(2 \cdot 3mm)} = 0.67Hz \tag{4}$$

where h_{max} is maximum excursion and v is maximum speed. As mentioned before we experimented with encapsulating the motors in both iron and mu metal to provide extra shielding. Because mu metal has a considerably higher permeability than iron, we wanted to check if this would affect the torque exerted by the motors. In both cases the tactels where run under different loads starting with 0 load and ending with the weight at which the motors did not respond consistently anymore. The mean values for the iron case under different loads are shown in Figure 13.

For iron we concluded that the maximum load a tactel could lift at maximum speed was 40

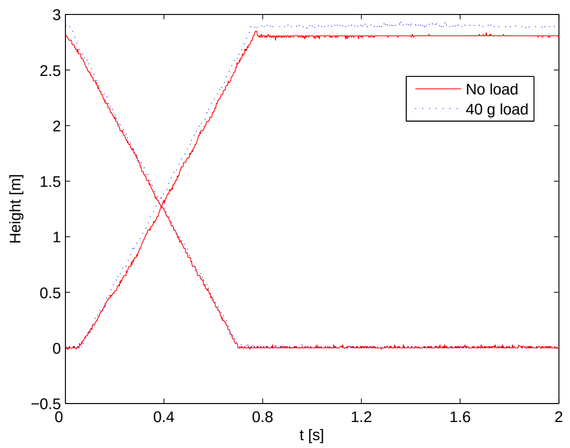

Figure 13: Plot showing step response under different loads when motors where encapsulated in iron.

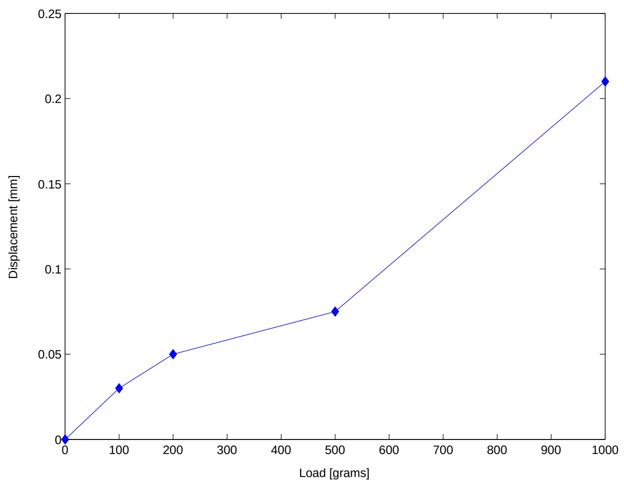

Figure 14: Plot showing stiffness of display.

grams, corresponding to approximately 0.4 N. Mu metal showed the same step response, but the maximum load at maximum speed increased to 50 grams. This indicates that using mu metal shielding does indeed increase the torque. The mu metal did also prove to be very effective as far as shielding is concerned. Note that at very low speeds we were able to lift up to 1 N when the motors were encapsulated in mu metal.

A 6 ms delay between command and pin movement was observed in performance trials.

3.3 Stiffness

To test the stiffness, we loaded a tactel with successive weights ranging from 100 grams to 1000 grams. The result is shown in Figure 14.

As the figure shows, the yield was only 0.21 mm with a load close to 10 N, hence we have a stiffness of close to 50 N/mm.

3.4 Friction

Estimating the friction is always challenging, and almost impossible without the actual device, although Richard, Cutkosky and MacLean present a method of identifying friction for haptic displays in [23].

We have based our friction estimates on the classic Coulomb friction model, where friction force is proportional to load [2]

$$F_f = \mu \cdot F_l \tag{5}$$

Here μ is the coefficient of friction and F_l is the normal force. There is also an initial static friction (stiction), $F_s = C$, that must be overcome for the motor to start rotating:

$$F_n = F_l + F_f + F_s = F_l + \mu F_l + C \tag{6}$$

Here F_n is the total force available for driving the mechanism, F_l is the load the tactel is actually able to lift and F_f the friction force (see Figure 15).

We know that

$$T_m \omega = F_n v \tag{7}$$

and

$$p\omega = v \tag{8}$$

where p is the screw pitch, ω is the motor's angular velocity and v is the linear velocity of the tactel. Hence we can estimate the friction constant for the screw mechanism from the following equation:

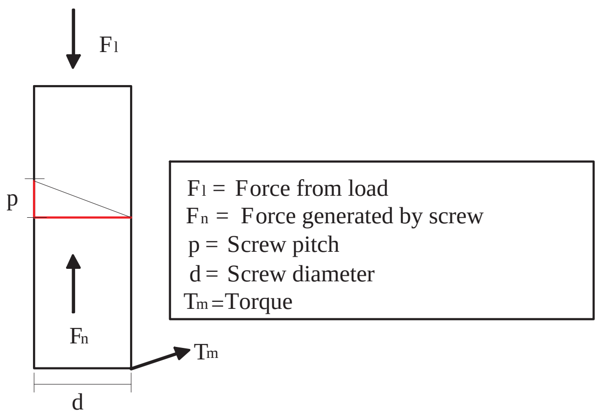

Figure 15: Forces and torques.

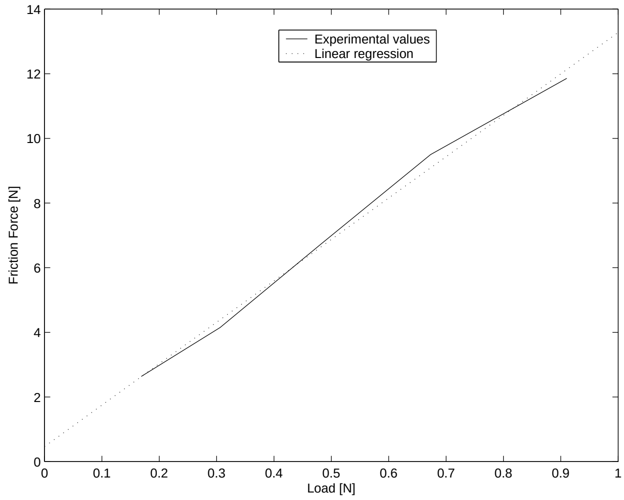

Figure 16: Load vs. friction, experimental values and polyfit.

$$T_m = I_m K_t - T_{fm} = T_l + T_f + T_s \\ = p[F_l(1+\mu) + C] \quad (9)$$

Here F_l is assumed to be the maximum load we can put on the tactel before the motor stalls. From experimental data we find a relationship between the voltage input to the motor and the maximum load a tactel can lift. Then we use these data to find a relationship between the torque and the load $[N]$. To estimate the friction we find how F_f varies with maximum load and use equation (9) to determine values for C and μ. This result is shown in Figure 16. Using linear regression we finally find that $C = 0.46$ and $\mu = 12.81$.

4 Discussion

Table 1 shows a comparison of different tactile displays [26], including our display.

Our display is small and has a size compatible with both the finger tip and the handle of a laparoscopic grasper. The number of pins can easily be increased, but this will result in a slight increase in size. The resolution would preferably have to be improved, but in our case it is restricted by the size of the motors. Both using smaller motors and a two-layer approach (where the top layer has shorter screws than the bottom layer, such that the motors can be stacked closer together) will increase the resolution significantly. The latter will, however, introduce other problems, such as different screw lengths or sluggishness. Changing the mechanism and introducing some sort of reorientation in the direction of applied force is also a possible option.

Theory corresponds well with reality for the bandwidth in that it follows the commanded velocity as long as the commutation is not too fast. If the motors cannot follow the input velocity, they slip and do not move at all. Despite this, the bandwidth of the display is well below the requirements introduced by Moy et al. [14]. There are several ways to increase the velocity, the most important being changing the gear head reduction and increasing the screws' thread pitch. The motors currently used are not available with a suitable gear head reduction to increase the bandwidth, while still providing a significant force on the finger tip. The same is the case when changing the screw pitch, as the forces will decrease both due to friction caused by the increased angle of attack between screw and nut, and the gear-up from increasing the thread pitch.

The maximum pin force at maximum speed is 0.5 N for our display, as opposed to the proposed

Table 1: Comparison of tactile displays (n.s = not stated).

Reference	Goal [14]	Ours	[25]	[1]	[14]	[27]	[3]	[4]	[20]
Actuator	n.s.	Servos		Pneumatic		SMA		Solenoid	
Array Size	10×10	4×8	6×6	4×4	5×5	1×10	8×8	8×8	20×20
Tactel Spacing[mm]	1	2.7	2	3.75	2.5	2	3.2	5	0.5
Temporal Bw.[Hz]	≥ 50	0.67	7.5/25	11	5	30	0.1	n.s.	40
Max Pin Force[N]	1	0.5	2	3	0.2	2	2.5	n.s.	1.3
Max Pin Height[mm]	4	3	2	5	0.6	3	3.5	1	2.5
Height Res.[mm]	0.4	0.04	0.1	n.s.	n.s.	0.1	n.s.	0.25	n.s.
Size[mm]	n.s.	$27\times20\times18$	76×119	$15\times15\times10$	n.s.	n.s	n.s.	n.s	n.s.

1 N in an ideal display. However, this is not as big a problem as the bandwidth limitations, so in later versions, maintaining this torque while increasing the bandwidth should be a priority.

From calculations we expected the positioning resolution to be 20 μm, but it was estimated to 40 μm from our performance tests. As can be seen in Figure 12, there is a dead zone in all trials in the first few position steps. The most likely reason for this can be explained by the left part of Figure 2, where the split in the screw is shown. As the hole that the bolt fits into is not circular, but rather slightly oval, this can result in commutations of the motor that do not cause any vertical motion. The dead zone is noticeable in all trials, and if this was accounted for when comparing with the linear case (by shifting the linear case to start at the point where vertical movement actually starts in the trials), it would have resulted in a higher positioning resolution. Another reason for the dead zone can be inaccuracies in the commutation scheme at start up. It was important to verify the positioning accuracy and repeatability, because the display does not provide position feedback. Introducing position sensors would require additional space, but would have been necessary if the tactels had been less accurate and repeatable. Despite this, putting too much load on the tactel could still introduce problems, since the control system can lose track of the motor's position. In such cases the motor must be recalibrated. Another disadvantage of the system is the price. The material price for the display housing and the tactel mechanism is not a problem, but manufacturing cost of the small parts might be considerable. The most expensive part of the system is the motors, which cost about 330 USD a piece. This is expected to be lower in the future.

The high stiffness of the display, which is an intrinsic property of the screw-based design, should be kept in later versions.

Since as much as 90 % of the torque can be lost to friction, better lubrication, polished screws or using more optimal materials such as teflon or ceramics, would probably improve the performance considerably.

To sum up, the major advantage of the system is the size and weight of the display combined with accurate positioning of the pins and high stiffness.

5 Conclusions and Future work

Although the bandwidth and force the reported display can provide are well below the ideal criteria posted by Moy et al. [14], we think that the design of this display is promising since it provides the opportunity to make small displays. Small stepper motors usually have the positioning resolution tactile displays require, and as we have seen we obtain very high stiffness using our design. Psychophysical experiments with the display were conducted in [19], and the results where promising, although there is a long way to go before tactile displays can render natural sensations.

Acknowledgements

The research was funded by the Research Council of Norway, grant 147830/320. Most of the assessment of the device was conducted at the Harvard Biorobotics laboratory, and the authors greatly appreciate the help and input from Professor Robert D. Howe and Dr. Christopher R. Wagner. We would also like to acknowledge the engineering workshop at the Department of Engineering Cybernetics, NTNU, for help with mechanical designs. Ragnhild Nesbakken at the Department of Product Design is acknowledged for the work on the laparoscopic handle. Finally we would like to thank Torgrim Gjelsvik at SINTEF IKT for major contributions to the design and making of the driver circuits.

References

[1] Darwin G. Caldwell, N. Tsagarakis, and C. Giesler. An integrated tactile/shear feedback array for stimulation of finger mechanoreceptor. In *Proceedings of the IEEE International Conference on Robotics and Automation*, pages 287–292, Detroit, MI, May 1999.

[2] Olav Egeland and Jan Tommy Gravdahl. *Modeling and Simulation for Automatic Control*. Marine Cybernetics, Trondheim, Norway, 2002.

[3] H. Fischer, R. Trapp, L. Schuele, and B. Hoffmann. Actuator array for use in minimally invasive surgery. *Journal de Physique IV (Colloque)*, 7:609–614, 1997.

[4] S. F. Frisken-Gibson, P. Bach-y-Rita, W. J. Tompkins, and J. G. Webster. A 64-solenoid, four-level fingertip search display for the blind. *IEEE Transactions on Biomedical Engineering*, BME-34:963–965, 1987.

[5] Michael Fritschi, Martin Buss, Knut Drewing, Regine Zopf, and Marc O. Ernst. Tactile feedback systems. Touch and Haptics Workshop at IEEE/RSJ International Conference on Intelligent Robots and Systems, Sendai, Japan, 2004.

[6] A. C. Guyton and J. E. Hall. *Textbook of Medical Physiology*. W.B. Saunders Company, tenth edition, 2000.

[7] Allan R. Hambley. *Electrical Engineering Principles and Applications*. Prentice Hall, second edition, 2002.

[8] Vincent Hayward and Juan Manuel Cruz-Hernández. Tactile display device using distributed lateral skin stretch. In *Symposium on Haptic Interfaces for Virtual Environment and Teleoperator Systems*, pages 1309–1314, Orlando, FL, Nov. 2000.

[9] Takayuki Iwamoto and Hiroyuki Shinoda. Ultrasound tactile display for stress field reproduction - Examination of non-vibratory tactile apparent movement. In *Proceedings of the First WorldHaptics Conference*, pages 220–228, Pisa, Italy, Mar. 2005.

[10] Hiroyuki Kajimoto, Naoki Kawakami, Susumu Tachi, and Masahiko Inami. SmartTouch: Electric skin to touch the untouchable. *IEEE Computer Graphics and Applications*, 24(1):36–43, Jan-Feb. 2004.

[11] S. J. Lederman and R. L. Klatzky. Sensing and displaying spatially distributed fingertip forces in haptic interfaces for teleoperator and virtual environment systems. *Presence: Teleoperators and Virtual Environments*, 8:86–103, 1999.

[12] J. M. Lee, C. R. Wagner, S. J. Lederman, and R. D. Howe. Spatial low pass filters for pin actuated tactile displays. In *Proceedings of the 11th International Symposium on Haptic Interfaces for Virtual Environment and Teleoperator Systems*, pages 57–62, Los Angeles, CA, 2003.

[13] Yasutoshi Makino and Hiroyuki Shinoda. Selective stimulation to superficial mechanoreceptors by temporal control of suction pressure. In *Proceedings of the First WorldHaptics Conference*, pages 229–234, Pisa, Italy, Mar. 2005.

[14] G. Moy, C. Wagner, and R. S Fearing. A compliant tactile display for teletaction. In *Proceedings of the IEEE International Conference on Robotics and Automation*, pages 3409–3415, San Francisco, CA, Apr. 2000.

[15] Ragnhild Nesbakken. Ergonomic guidelines in handle design - The challenges of laparoscopic surgical instruments. Student project report, NTNU, 2004.

[16] Maria V. Ottermo. *Virtual Palpation Gripper*. PhD thesis, NTNU, 2006.

[17] Maria V. Ottermo, Marit Øvstedal, Thomas Langø, Øyvind Stavdahl, Yunus Yavuz, Tor A. Johansen, and Ronald Mårvik. The role of tactile feedback in laparoscopic surgery. *Surgical Laparoscopy, Endoscopy & Percutaneous Techniques*, 16(6):390–400, Dec 2006.

[18] Maria V. Ottermo, Øyvind Stavdahl, and Tor A. Johansen. Electromechanical design of a miniature tactile shape display for minimally invasive surgery. In *Proceedings of the First World-Haptics Conference*, pages 561–562, Pisa, Italy, Mar. 2005.

[19] Maria V. Ottermo, Øyvind Stavdahl, and Tor A. Johansen. A remote palpation instrument for laparoscopic surgery: Design and performance. In *Biomedical Engineering Society Annual Meeting*, Chicago, IL, 2006.

[20] D. T. V. Pawluk, C. P. van Buskirk, J. H. Killebrew, S. S. Hsiao, and K. O. Johnson. Control and pattern specification for a high density tactile array. In *Proceedings of the ASME Dynamic Systems and Control Division*, volume 64, pages 97–102, New York, USA, 1998.

[21] W. J. Peine, P. S. Wellman, and R. D. Howe. Temporal bandwidth requirements for tactile shape displays. In *Proceedings of the Symposium on Haptic Interfaces for Virtual Environment and Teleoperator Systems, ASME International Mechanical Engineering Congress and Exposition*, pages 107–113, Dallas, TX, Nov 1997.

[22] William Jeane Peine. *Remote Palpation Instruments for Minimally Invasive Surgery*. PhD thesis, Harvard University, Cambridge, MA, Oct. 1998.

[23] Christopher Richard, Mark R. Cutkosky, and Karon MacLean. Friction identification for haptic display. In *Proceeding of the 1999 ASME IMECE*, Nashville, TN, Nov. 1999.

[24] I. Sarakoglou, N. Tsagarakis, and D. G. Caldwell. A portable fingertip tactile feedback array - Transmission system reliability and modelling. In *Proceedings of the First WorldHaptics Conference*, pages 547–548, Pisa, Italy, Mar. 2005.

[25] Christopher R. Wagner, S. J. Lederman, and Robert D. Howe. A tactile shape display using RC servomotors. In *Proceedings of the Tenth International Symposium on Haptic Interfaces for Virtual Environment and Teleoperator Systems*, pages 354–356, Orlando, USA, Mar. 2002.

[26] Christopher R. Wagner, S. J. Lederman, and Robert D. Howe. Design and performance of a tactile shape display using RC servomotors. *Haptics-e: The Electronic Journal of Haptic Research*, 3(4), Aug. 2004.

[27] P. S. Wellman, W. J. Peine, G. E. Favalora, and R. D. Howe. Mechanical design and control of a high-bandwidth shape memory alloy tactile display. In *International Symposium on Experimental Robotics*, Barcelona, Spain, Jun. 1997.